Parametric interactions in the organic salt 4-N,N-dimethylamino-4′-N′-methyl-stilbazolium tosylate at telecommunication wavelengths

U. Meier, M. Bösch, Ch. Bosshard, F. Pan, and P. Günter

Citation: J. Appl. Phys. **83**, 3486 (1998); doi: 10.1063/1.366560
View online: http://dx.doi.org/10.1063/1.366560
View Table of Contents: http://jap.aip.org/resource/1/JAPIAU/v83/i7
Published by the American Institute of Physics.

Parametric interactions in the organic salt 4-*N*,*N*-dimethylamino-4′-*N*′-methyl-stilbazolium tosylate at telecommunication wavelengths

U. Meier,[a] M. Bösch, Ch. Bosshard, F. Pan,[b] and P. Günter
Nonlinear Optics Laboratory, Institute of Quantum Electronics, ETH Hönggerberg, CH-8093 Zürich, Switzerland

(Received 24 October 1997; accepted for publication 22 December 1997)

We show that the organic salt 4-*N*,*N*-dimethylamino-4′-*N*′-methyl-stilbazolium tosylate, originally developed for electro-optic applications, is also a very interesting material for phase-matched parametric interactions such as frequency-doubling and optic parametric oscillation in the near infrared. These favorable properties are due to the large off-diagonal element d_{26} which gives measured effective phase-matchable nonlinear optical coefficients of $d_{\text{eff}}=31\pm5$ and 15 ± 3 pm/V at the telecommunication wavelengths of $\lambda=1313$ and 1535 nm, respectively. © *1998 American Institute of Physics.* [S0021-8979(98)03507-5]

I. INTRODUCTION

Organic salts based on strong Coulomb interactions between charged molecules often show noncentrosymmetric packing as, e.g., in 4-dimethylamino-*N*-methylstilbazolium salts.[1] There are several successful examples of a noncentrosymmetric crystal packing in molecular salts.[2–4] The material with the largest second-order nonlinearities in this class is 4-*N*,*N*-dimethylamino-4′-*N*′-methyl-stilbazolium tosylate (DAST).[4,5] DAST crystals are very interesting especially for electro-optic applications due to the exceptionally large nonlinear optical susceptibilities and the good alignment of the chromophores in the crystal. [5–7] The almost electronic origin of the electro-optic effects was confirmed[8] and photorefractive effects in the near infrared were reported.[9] Due to the almost parallel alignment of the stilbazolium cations (angle of 20° between the charge-transfer axis and the polar crystal axis a) DAST was believed to be less suitable for phase-matched parametric interactions such as, e.g., frequency doubling where in the simplest approximation the chromophores should be arranged at 55° with respect to the polar axis for optimum optical frequency conversion for the most important point groups.[10]

In this work, we show that even the unfavorable orientation of the molecules in DAST leads to a large effective phase-matchable nonlinear optical coefficient for sum- and difference-frequency conversion. This is due to a large nonlinear optical coefficient d_{212}. We present our results on dispersion measurements of the largest nonlinear optical coefficients d_{111}, d_{122}, and d_{212} and show the potential of DAST for parametric interactions through phase-matched second-harmonic generation experiments around the telecommunication wavelengths at $\lambda=1300$ and 1500 nm. Our experimental results of highly efficient phase-matched frequency doubling at these wavelengths make DAST also an interesting material for cascaded second-order nonlinearities.[11–13]

[a]Electronic mail: urs.meier@iqe.phys.ethz.ch
[b]Present address: Molecular OptoElectronics Corp. (MOEC), 877 25th Street, Watervliet, New York 12189.

II. NONLINEAR OPTICAL SUSCEPTIBILITIES

The DAST crystals used for the determination of the nonlinear optical susceptibilities d_{ijk} and the type II phase matching measurements described below have been grown by the temperature lowering method.[14] DAST belongs to the point group m. The angles between the dielectric principal axes x_1 and x_3 and the crystallographic axes a and c are 5.4° and 3.2°, respectively.[15] The x_2 axis is along the b axis. The polar axis of the crystal is along x_1. The existing nonlinear optical coefficients are therefore d_{111}, d_{122}, d_{133}, d_{131}, d_{232}, d_{212}, d_{311}, d_{322}, d_{333}, and d_{313}.

A. Experimental details

The nonlinear optical susceptibilities d_{ijk} were determined by the standard Maker fringe technique.[16] The fundamental wavelengths used for the Maker fringe measurements were $\lambda=1318$ [Nd:yttrium aluminum–garnet (YAG) laser B.M.I., 15 ns, Q switched at 30 Hz], 1542 (first Stokes-line generated in a high pressure Raman cell filled with methane and pumped by a Surelite Nd:YAG laser at $\lambda=1064$ nm, 7 ns, Q switched at 2 Hz), and 1907 nm (first Stokes-line generated in a high pressure Raman cell filled with H_2 and pumped by the same laser). The measured second-harmonic intensities were corrected for absorption losses using the experimentally determined absorption coefficients, and compared to a quartz reference using the new reference value ($d_{111}=0.29$ pm/V at $\lambda=1318$ and 1542 nm, $d_{111}=0.28$ pm/V at $\lambda=1907$ nm, all based on $d_{111}=0.30$ pm/V at $\lambda=1064$ nm[17] and the Miller-δ[18] to account for the wavelength dispersion). The samples used were all c plates (according to the dielectric axis) with different thicknesses between 350 and 450 μm. The crystals were oriented with their dielectric x_1 axis along the rotation axis of the Maker Fringe experiment. This geometry allowed the determination of the coefficients d_{111}, d_{122}, and d_{212} which are summarized in Table I.

B. Results and discussions

The large diagonal nonlinear optical coefficient d_{111} of DAST [e.g., $d_{111}=1040\pm110$ pm/V at $\lambda=1318$ nm (reso-

TABLE I. Second-order nonlinear optical coefficients d_{ijk} (pm/V) and coherence lengths l_c (μm) of DAST. The reference value d_{111}^Q of α quartz is given for completeness.

λ (nm)	d_{111}	l_c^{111}	d_{122}	l_c^{122}	d_{212}	l_c^{212}	d_{111}^Q
1318	1010 ± 110	0.64 ± 0.02	96 ± 9	0.30 ± 0.02	53 ± 12	3.9 ± 0.8	0.292
1542	290 ± 15	1.38 ± 0.05	41 ± 3	0.48 ± 0.01	39 ± 2	2.50 ± 0.02	0.286
1907	210 ± 55	3.2 ± 0.3	32 ± 4	0.67 ± 0.03	25 ± 3	2.1 ± 0.2	0.277

nance enhanced)] is due to the good alignment of the charge-transfer axes of the cation along x_1. The absorption of DAST is strongly anisotropic: the absorption edge for light polarized along the dielectric x_1, x_2, and x_3 directions (defined here for an absorption coefficients of $5\,\mathrm{cm}^{-1}$) are at $\lambda=700$, 650, and 590 nm, respectively.[14] For these reasons, the Kleinman symmetry[19] is no longer valid for short fundamental wavelengths (see d_{122} and d_{212} in Table I that are approximately equal at 1542 and 1907 nm but differ by almost a factor of two at $\lambda=1318$ nm).

A strong resonance enhancement of the nonlinear optical coefficients d_{111} and d_{122} was found as we approach the absorption region of DAST. The strong absorption anisotropy is favorable for phase-matched second-harmonic generation in the near infrared since one can take advantage of large nonlinear optical coefficients with a second-harmonic polarization in the x_1-x_3 plane (using d_{212} at angles of incidence near 45°) therefore reducing the absorption at the second harmonic (see below).

III. PHASE MATCHED PARAMETRIC INTERACTION

Due to the favorable dispersion of the refractive indices of DAST, phase matched second-harmonic generation and parametric generation are possible for types I and II configurations. Using the measured refractive indices,[6,15] we calculated the directions of the wave vectors $\mathbf{k}_i$ of the interacting waves in the crystal for which the phase matching conditions are fulfilled: $\omega_3=\omega_1+\omega_2$ and $\mathbf{k}_{\omega_3}=\mathbf{k}_{\omega_1}+\mathbf{k}_{\omega_2}$.

For collinear parametric interaction, where all $\mathbf{k}_i$ are parallel to one another, the phase matching condition is $n(\omega_3)=n(\omega_1)\omega_1+n(\omega_2)\omega_2$. $n(\omega_i)$ are the refractive indices of the waves of frequency ω_i. The nonlinear polarization for general directions in the crystal can be written as

$$|P^{\omega_3}|=2\epsilon_0 d_{\mathrm{eff}}|E^{\omega_1}||E^{\omega_2}| \quad \text{(sum-frequency generation)}, \tag{1}$$

$$|P^{2\omega}|=\epsilon_0 d_{\mathrm{eff}}|E^{\omega}|^2 \quad \text{(type I second-harmonic generation)}, \tag{2}$$

$$d_{\mathrm{eff}}=\sum_{ijk} d_{ijk}^{(\omega_3,\omega_1,\omega_2)}\cos(\alpha_i^{\omega_3})\cos(\alpha_j^{\omega_1})\cos(\alpha_k^{\omega_2}), \tag{3}$$

where d_{eff} is the effective nonlinear optical coefficient, α_i^{ω} are the angles between the electric field vector $\mathbf{E}^{\omega}$ of the wave with frequency ω and the main axis i of the indicatrix.[20,21] Note, that the walk-off angle ρ between the wave vector and the Poynting vector has been taken into account to calculate the electric field vectors and the α_i^{ω}.

Figure 1 shows the propagation directions (in spherical coordinates θ, ϕ) for which phase-matched second-harmonic generation occurs in DAST crystals. Due to large birefringence in the transparent spectral region of DAST, noncritical, phase matching cannot be achieved. The optimum conditions for second-harmonic generation in DAST exist for type II phase matching with $\phi=0°$. As an example, we can cover a wavelength range of 1300–1500 nm with $\theta=28°-45°$. Figure 2 shows the theoretical values of the phase-matching loci, effective nonlinear optical coefficients, and walk-off angles for $\lambda=1318$ and 1542 nm. For $\phi=0°$ and $\lambda=1318$ and 1542 nm, the phase matching angles are $\theta=30°$ and 46° with walk-off angles of $\rho=17°$ and 16° giving effective nonlinear coefficients of $d_{\mathrm{eff}}=36.8$ and 18.8 pm/V, respectively. The wavelength deviation of d_{eff} to the actual phase-matching experiments presented below ($\lambda=1313$ and 1535 nm) can be neglected.

A. Experimental details

We determined the second-harmonic generation efficiency and the effective nonlinear optical coefficient d_{eff} by comparing the phase-matched signals of DAST with those of a $KNbO_3$ crystal using cw lasers [diode pumped cw Nd:YLF laser (ADLAS model DPY 203C) at 1313 nm and a cw micro laser (Amoco model 1.5-EHA) at 1535 nm] and compared them with our theoretical predictions. According to the phase matching calculations, the DAST crystals were cut with the polished faces perpendicular to the direction $\phi=0°$ and $\theta=45°\pm2°$, (101) faces, to be able to measure phase-matched second-harmonic generation at the wavelengths $\lambda=1313$ and 1535 nm (see below) with the same crystals. The crystal thicknesses were varied ($L=0.480$, 1.125, 3.183 nm) in order to investigate the influence of the large walk-off angle ρ. The $KNbO_3$ crystal was a 1 mm (011)

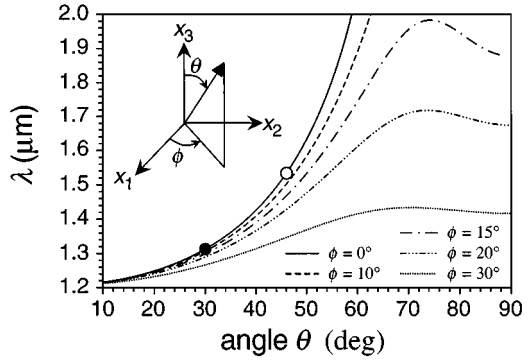

FIG. 1. Propagation directions (in spherical coordinates θ,ϕ) for type II phase-matched second-harmonic generation in single crystals of DAST. $\phi=0°$: rotation axis is x_2, polarization of the pump beam is at 45° to x_2, the polarization of the second harmonic is along x_2.

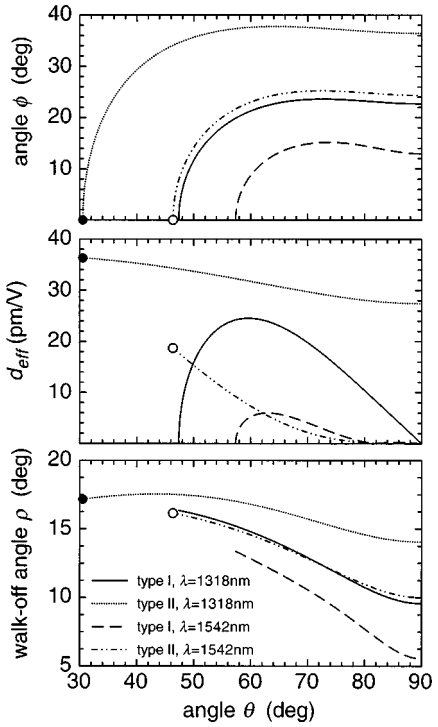

FIG. 2. Phase-matching loci (theoretical values), effective nonlinear optical coefficients, and walk-off angles for $\lambda=1318$ and 1542 nm. ● and ○ indicate the values where the actual experiments were carried out. $\phi=0°$: rotation axis is x_2, polarization of the pump beam is at 45° to x_2, the polarization of the second harmonic is along x_2.

plate with $d_{\text{eff}}=9.6$ pm/V at 1313 nm and 8.7 pm/V at 1535 nm (based on measured nonlinear optical coefficients,[22] the Miller-δ,[18] and phase-matching calculations).[23]

B. Results and discussion

The phase-matching measurements were performed with the lasers described above in the setup shown in Fig. 3 using a lock-in amplifier (Stanford Research) to measure the second-harmonic signal. The experimental results are summarized in Table II. We measured values of d_{eff} that were more than three times larger ($\lambda=1313$ nm) and 1.7 times

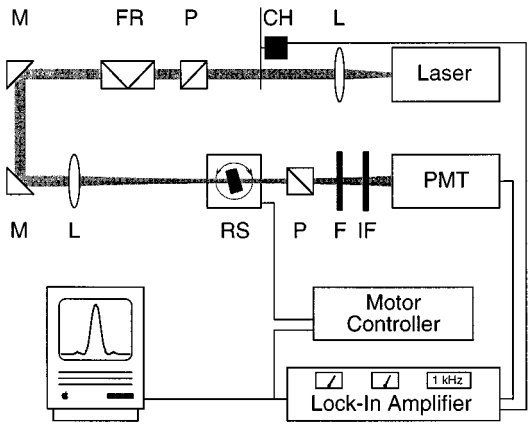

FIG. 3. Experimental setup for the phase-matching measurements. The beam radius was varied by using different lenses. L, lens; CH, chopper; P, polarizer; FR, fresnel rhombus; M, mirror; RS, rotation stage; F, filter; IF, interference filter; PMT, photomultiplier.

larger ($\lambda=1535$ nm) than $KNbO_3$. Even at $\lambda=1313$ nm, there was no noticeable absorption at the second-harmonic wavelength since the second-harmonic wave is polarized in the x_1-x_3 plane where no intrinsic absorption is present. Our values are also in good agreement with the ones calculated from the measured nonlinear optical coefficients. The results in Table II show the influence of both the walk-off angle ρ and the acceptance angle $\delta\theta$ defined by $\Delta kL/2=\pi$ ($\Delta k=k^{2\omega}-k_1^{\omega}-k_2^{\omega}$) on the second-harmonic efficiency. For small beam radii (e.g., $w_0=75$ μm for $\lambda=1313$ nm), we see that a decrease of the sample thickness L leads to larger values of d_{eff} since L is closer to the walk-off length $L_\rho=\sqrt{\pi}w_0/\rho=450$ μm. For the same reason, increasing w_0 also leads to larger values of d_{eff}. As a further example, for $w_0=210$ μm ($\lambda=1313$ nm), the ratio $I^{2\omega}_{\text{DAST}}/I^{2\omega}_{\text{KNbO}_3}$ first increases with decreasing thickness due to a better beam overlap and then decreases on further reducing L due to the expected thickness dependence of $I^{2\omega}$. For small w_0, the measured acceptance angles are almost independent of the crystal thickness L and larger than the theoretically calcu-

TABLE II. Results of the phase-matched second-harmonic generation experiments in DAST (d_{eff} in pm/V, crystal thickness L in mm, beam radius w_o (Gaussian beam) in μm, acceptance angles $\delta\theta$ in deg). The experimental errors are w_o: 1%–3%, d_{eff}:10%, $\delta\theta$: 1%–2%.

	$\lambda=1313$ nm					$\lambda=1535$ nm				
L	w_o	$\frac{I^{2\omega}_{\text{DAST}}}{I^{2\omega}_{\text{KNbO}_3}}$	d_{eff}	$\delta\theta$ (exp)	$\delta\theta$ (theor.)	w_o	$\frac{I^{2\omega}_{\text{DAST}}}{I^{2\omega}_{\text{KNbO}_3}}$	d_{eff}	$\delta\theta$ (exp)	$\delta\theta$ (theor.)
3.183		4.7	2.5	0.81	0.090		6.6	2.2	0.67	0.094
1.125	75	9.5	8.7	0.84	0.25	92	7.4	6.2	0.64	0.26
0.480		10.4	20	0.82	0.60		4.2	11	0.82	0.62
3.183		43	7.6	0.24	0.090		35	5	0.25	0.094
1.125	210	56	21	0.29	0.25	180	23	11	0.34	0.26
0.480		24	31	0.56	0.60		7.1	14	0.72	0.62
3.183		170	15	0.18	0.090		190	12	0.19	0.094
1.125	820	80	25	0.25	0.25	750	48	16	0.30	0.26
0.480		24	31	0.57	0.60		8.6	15	0.72	0.62
d_{eff} from theory:			36			d_{eff} from theory:		18		

lated ones. This arises most likely from the fact that the beam divergence is similar to the acceptance angle for small w_0 leading to a broadening of the phase-matching curves dominated by the beam divergence. For larger w_0 we get the expected dependence of $\delta\theta$ on the sample thickness and a good agreement between experiment and theory (Table II).

IV. CONCLUSION

In conclusion, we have determined the nonlinear optical coefficients d_{111}, d_{122}, and d_{212} of the organic salt DAST as a function of wavelength. We have shown that there exist phase-matching configurations for frequency doubling with large effective nonlinear optical coefficients at telecommunication wavelengths which is interesting for applications such as, e.g., the cascading of second-order nonlinearities[11–13] and optic parametric oscillation. The theoretical calculations were confirmed by the first phase-matched optical frequency-doubling experiments at the telecommunication wavelengths around $\lambda=1300$ and 1500 nm. Figures of merit for frequency conversion, $d_{\text{eff}}^2/n^3=230\ \text{pm}^2/\text{V}^2$ at $\lambda=1313$ nm, that are almost 30 times higher than that of $KNbO_3$ ($KNbO_3$:7.9 pm^2/V^2) or 120 times higher than that of $KTiPO_4$ (KTP:1.9 pm^2/V^2) were measured, all values adjusted to the same reference value of d_{111} of α quartz. The large nonlinear optical coefficients of DAST allow efficient frequency conversion close to the absorption edge due to the huge absorption anisotropy.

ACKNOWLEDGMENTS

We thank J. Hajfler for his expert sample preparation. This work has been supported by the Swiss National Science Foundation.

[1] G. R. Meredith, in *Nonlinear Optical Properties of Organic and Polymeric Materials*, ACS Symposium Series, Vol. 233, edited by D. J. Williams (American Chemical Society, Washington, D.C., 1983), p. 27.
[2] S. Okada, A. Masaki, H. Matsuda, H. Nakanishi, T. Koike, T. Ohmi, and N. Yoshikawa, Proc. SPIE **1337**, 178 (1990).
[3] S. Okada, A. Masaki, H. Matsuda, H. Nakanishi, M. Koto, R. Muramatsu, and M. Otsuka, Jpn. J. Appl. Phys., Part 1 **29**, 1112 (1990).
[4] S. R. Marder, J. W. Perry, and W. P. Schaeffer, Science **245**, 626 (1989).
[5] S. R. Marder, J. W. Perry, and C. P. Yakymyshyn, Chem. Mater. **6**, 1137 (1994).
[6] F. Pan, G. Knöpfle, Ch. Bosshard, S. Follonier, R. Spreiter, M. S. Wong, and P. Günter, Appl. Phys. Lett. **69**, 13 (1996).
[7] Ch. Bosshard, G. Knöpfle, P. Prêtre, S. Follonier, C. Serbutoviez, and P. Günter, Opt. Eng. (Bellingham) **34**, 1951 (1995).
[8] R. Spreiter, Ch. Bosshard, F. Pan, and P. Günter, Opt. Lett. **22**, 564 (1997).
[9] S. Follonier, Ch. Bosshard, F. Pan, and P. Günter, Opt. Lett. **21**, 1655 (1996).
[10] J. Zyss and J. L. Oudar, Phys. Rev. A **26**, 2028 (1982).
[11] G. I. Stegeman, M. Sheik-Bahae, E. Van Stryland, and G. Assanto, Opt. Lett. **18**, 13 (1993).
[12] G. I. Stegeman, D. J. Hagan, and L. Torner, J. Opt. Quant. Electron. **28**, 1691 (1996).
[13] Ch. Bosshard, Adv. Magn. Reson. **8**, 385 (1996).
[14] F. Pan, M. S. Wong, Ch. Bosshard, and P. Günter, Adv. Magn. Reson. **8**, 592 (1996).
[15] G. Knöpfle, R. Schlesser, R. Ducret, and P. Günter, Nonlinear Opt. **9**, 143 (1995).
[16] J. Jerphagnon and S. K. Kurtz, J. Appl. Phys. **41**, 1667 (1970).
[17] D. A. Roberts, IEEE J. Quantum Electron. **28**, 2057 (1992).
[18] R. C. Miller, Appl. Phys. Lett. **5**, 17 (1964).
[19] D. A. Kleinman, Phys. Rev. **126**, 1977 (1962).
[20] F. Brehat and B. Wyncke, J. Phys. B **22**, 1891 (1989).
[21] B. Wyncke and F. Brehat, J. Phys. B **22**, 363 (1989).
[22] J.-C. Baumert, J. Hoffnagle, and P. Günter, in *1984 European Conference on Optics, Optical Systems, and Applications* (SPIE, Amsterdam, 1984), p. 374.
[23] I. Biaggio, P. Kerkoc, L.-S. Wu, P. Günter, and B. Zysset, J. Opt. Soc. Am. B **9**, 507 (1992).